Supporting Information for "Bubble mediated gas transfer and gas transfer limitation of DMS and CO_2"

A. Zavarsky[1]*, L. Goddijn-Murphy[2], T. Steinhoff[1], and C. A. Marandino[1]

[1]GEOMAR Helmholtz-Centre for Ocean Research Kiel, Kiel, Germany

[2]University of the Highlands and Islands

Contents

Motion correction

The correction of the 3-D wind speeds measured by the sonic anemometer was based upon *Miller et al.* [2010]; *Edson et al.* [1998]; *Landwehr et al.* [2015]. The motion of the ship is measured with an intertial motion unit (IMU) and is subtracted from the measured wind speed. Figure 1 shows a power spectrum of the vertical wind. The black line shows the uncorrected raw, as measured, vertical wind power spectrum. Clearly visible is a peak around 0.2 Hz, which originates from the motion of the ship in the wave field. The red line illustrates the motion corrected vertical wind power spectrum. The dashed line shows the expected $-\frac{2}{3}$ decay of the turbulent power spectrum (TPS) in the inertial subrange [*Kolmogorov*, 1941] (Equation 1). Originally, as porposed by Kolomogorov, the decay is relative to $f^{-\frac{5}{3}}$, but Figure 1 shows $f \cdot TPS$ (Equation 1) and, as a consequence, the decay is proportional to $-\frac{2}{3}$.

*Metzstraße, Kiel, Germany

Corresponding author: Alex Zavarsky, alexz@mailbox.org

$$TPS \propto f^{-\frac{5}{3}} \cdot f \longrightarrow TPS \propto f^{-\frac{2}{3}} \tag{1}$$

Post processing

Eddy covariance data must be corrected for the delay between gas and wind measurements, as well as high frequency fluctuation losses in the tubing. We use a regular valve switch of an isotopically labeled standard to correct both issues. An ideal valve switch is a rectangular function. The tube's low-pass filter behavior alters the ideal rectangular signal as well as the turbulence in the tube. Therefore, we applied a low-pass filter to an ideal rectangle signal, in order to fit the shape of the measured isotopically labeled gas concentration over time. Figure 2 shows an ideal valve switch, the actual measured valve switch and the output of the low-pass filter applied to the ideal valve switch. The loss in high frequency power, displayed by the low-pass filter, is equal to the loss of high frequency fluctuations in the 1/2" Teflon tube connecting the air-intake to the laboratory container. Using the parameters from the low-pass filter we can put a gain factor on the cospectra. The loss displayed a linear relationship with 10 m neutral wind speed u_{10n}. The gain factors for DMS G_{DMS} and CO_2 G_{CO_2} can be seen in equation (2).

$$\begin{aligned} G_{DMS} &= 1.032 + 0.0021 \cdot u_{10} \\ G_{CO_2} &= 1.0128 + 0.0021 \cdot u_{10} \end{aligned} \tag{2}$$

All data points were then multiplied by the gain factor using their respective u_{10n} wind speed.

To get a right time synchronization of the concentration fluctuation c' and the vertical wind fluctuation w', we first set the time delay to the value obtained from the delay tests. Then, to increase the delay precision, we cross correlated the recorded wind w' and the respective air concentration c'. This was done by shifting the two data sets by 0.1 s steps and setting the delay to the maximum correlation (flux out of the ocean) or a minimum correlation (flux into the ocean). The maximum possible offset was set to ±1 s. Figure 3 shows on the x-axis the shifting of the delay time in relation to the delay test time. The y-axis shows the correlation. As the DMS flux is out of the ocean, in this example, we set the delay offset to the value of the maximum correlation. In the example of Figure 3 this was -0.3 s.

DMS and CO_2 spectra and cospectra

Figures 4 and 5 show a power spectrum of measured DMS and CO_2 concentrations. Additionally, a reference line shows the $-\frac{2}{3}$ decay. The original Kolmogorov [*Kolmogorov*, 1941] decay is $-\frac{5}{3}$, but as $f \cdot power$ is shown $f^{-\frac{5}{3}} \cdot f \longrightarrow f^{-\frac{2}{3}}$. Figures 6 and 7 show a cospectrum of the covariance c'w' between the fluctuation of the vertical wind speed and the concentration fluctuation for CO_2 and DMS, respectively. We fitted an empirical function, Equation 3, proposed by *Kaimal et al.* [1972] to the measured data as a quality reference. a and b are the fitting parameters.

$$C_{cw}(f) = \frac{a \cdot f}{(1 + b \cdot f)^{2.4}} \quad \text{for } f \geq 0.22$$
$$C_{cw}(f) = \frac{a \cdot f}{(1 + b \cdot f)^{1.75}} \quad \text{for } f \leq 0.22 \tag{3}$$

Ship data outage

Figure 8 shows the uncorrected wind speed measured by the ship's meteorological station. Between DOY 209.25 and DOY 211.75 data outages in the measurements of wind speed and wind direction occurred. These outages, if longer than 30 min, were filled with data from the eddy covariance measurement system.

CO_2 data discard

Figure 9 shows the full CO_2 gas transfer velocity data set. We discarded CO_2 gas transfer velocities below -20 cm h^{-1} and above 80 cm h^{-1}. These values are marked by the two horizontal black lines.

During this cruise the ΔpCO_2 value changed sign three times. This means that we also measured in very low ΔpCO_2 environments, which increases the likelihood of these extreme values. In our opinion the discarded data points did not have matching flux and ΔpCO_2 values. The reasons could [1] be that the flux footprint is different than the point of the ΔpCO_2 measurement [2] a difference between the ocean surface ΔpCO_2 and the value measured at 5 m depth in the moon pool [3] measurement uncertainty in the ΔpCO_2 value. At such low ΔpCO_2 values, a slight change can cause these extreme k values. Therefore these are discarded. There are also low ΔpCO_2 gas transfer velocities (Figure 9) which do not show extreme values. These data points may not suffer from the three points made earlier and are therefore kept in the data set.

Table 1. Fit coefficients [p_0, p_1, p_2, p_3] for $y = p_0 + p_1 \cdot u_{10} + p_2 \cdot u_{10}^2 + p_3 \cdot u_{10}^3$. Measured indicates the Indian Ocean field data (for CO_2 only k_{660} values between -10 and 80 cm h^{-1} were included). Δd_i is the error estimation based on Equation 22. Hybrid model is calculated using 'independent bubble model' [*Woolf*, 1997] and the MAP, MM and SP W-parameterizations as described in Section 2.3 .

y	p_0	Δd_0	p_1	Δd_1	p_2	Δd_2	p_3	Δd_3
k_{water} CO_2 MEASURED	-7	±20	4	±8	-0.1	±0.9	0.01	±0.03
k_{water} DMS MEASURED	-12	±12	6	±4	-0.3	±0.5	0.00	±0.02
Δk_{water} MEASURED	5	±23	-2	±9	0.15	±1.0	0.00	±0.04
k_{b,CO_2} MODEL MAP	0.07	±0.04	0.22	±0.02	0.027	±0.002	0.0033	±0.0001
k_{b,CO_2} MODEL MM	-1.64	±0.08	0.62	±0.03	-0.123	±0.004	-0.0042	±0.0001
k_{b,CO_2} MODEL SP	-2.90	±0.05	1.92	±0.02	-0.422	±0.002	0.0313	±0.0001

The DMS gas transfer velocities did not contain such extreme values. The reason could be that DMS air-sea gradient concentration always showed a sufficient magnitude.

Polynomial fits to CO_2 and DMS data

Table 1 shows the fits described in Section 3.6 of the main manuscript. The errors Δd_i are to large to confirm a significant difference between the CO_2 and DMS data. k_{b,CO_2} from MAP, MM and SP are shown in Figure 14 in the main manuscript.

References

Edson, J. B., A. A. Hinton, K. E. Prada, J. E. Hare, and C. W. Fairall (1998), Direct covariance flux estimates from mobile platforms at sea, *Journal of Atmospheric and Oceanic Technology*, *15*(2), 547–562, doi:10.1175/1520-0426(1998)015<0547:dcfefm>2.0.co;2.

Kaimal, J. C., J. C. Wyngaard, Y. Izumi, and O. R. CotÃľ (1972), Spectral characteristics of surface-layer turbulence, *Quarterly Journal of the Royal Meteorological Society*, *98*(417), 563–589, doi:10.1002/qj.49709841707.

Kolmogorov, A. N. (1941), The local structure of turbulence in incompressible viscous fluid for very large reynolds numbers, in *Dokl. Akad. Nauk SSSR*, vol. 30, pp. 299–303.

Landwehr, S., N. O'Sullivan, and B. Ward (2015), Direct flux measurements from mobile platforms at sea: Motion and airflow distortion corrections revisited, *Journal of Atmosp-*

heric and Oceanic Technology, *32*(6), 1163–1178, doi:10.1175/jtech-d-14-00137.1.

Miller, S. D., C. Marandino, and E. S. Saltzman (2010), Ship-based measurement of air-sea co2 exchange by eddy covariance, *Journal of Geophysical Research: Atmospheres*, *115*(D2), n/a–n/a, doi:10.1029/2009JD012193.

Woolf, D. K. (1997), Bubbles and their role in gas exchange, in *The Sea Surface and Global Change:*, edited by P. S. Liss and R. A. Duce, pp. 173–206, Cambridge University Press, Cambridge, doi:10.1017/CBO9780511525025.007.

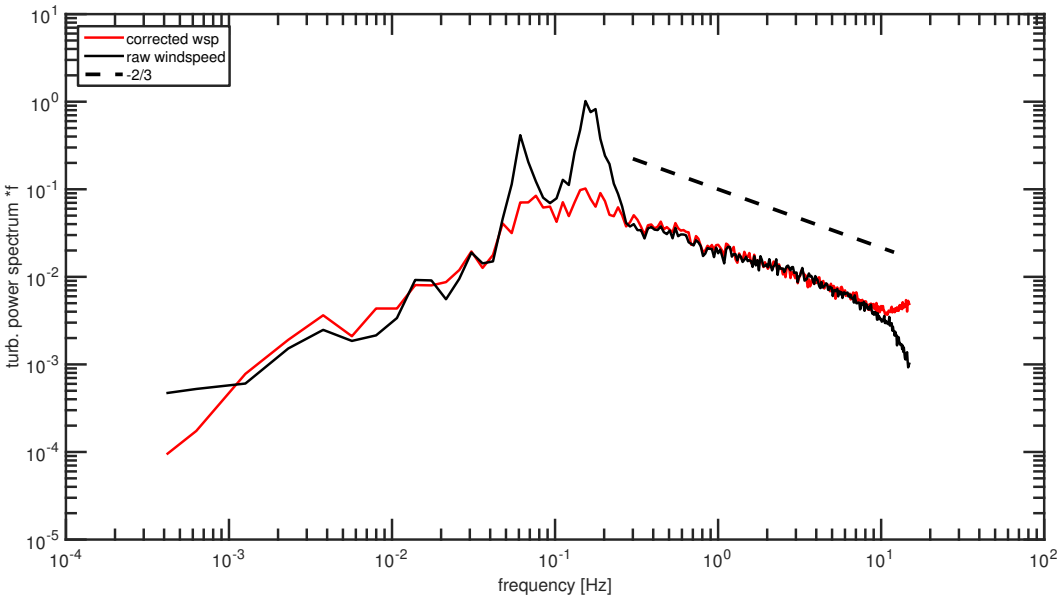

Figure 1. A sample vertical wind w' power spectrum before the correction (black) and after the correction (red). The dashed line is a reference to the $-\frac{2}{3}$ decay in the inertial subrange.

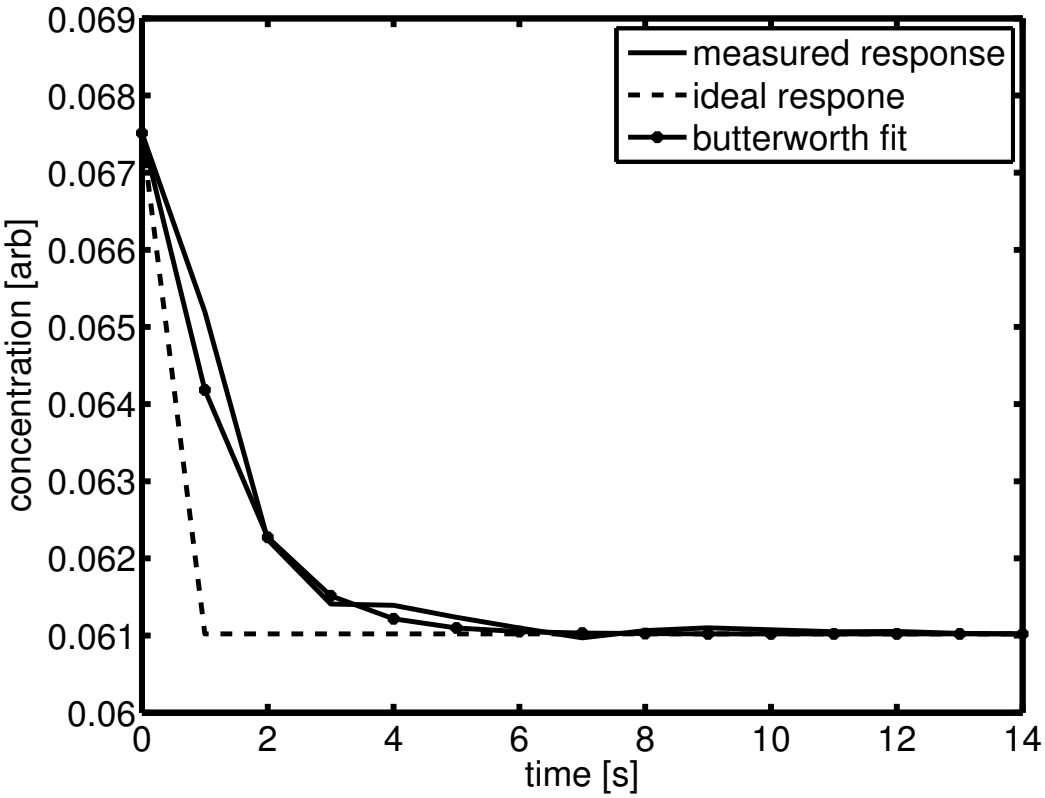

Figure 2. The concentration of the isotopically labeled reference gas during a valve switch. We applied and tuned a low-pass filter to an ideal valve switch to match the measured progression. Using the low-pass filter parameters, we accounted for the high frequency loss in the tube.

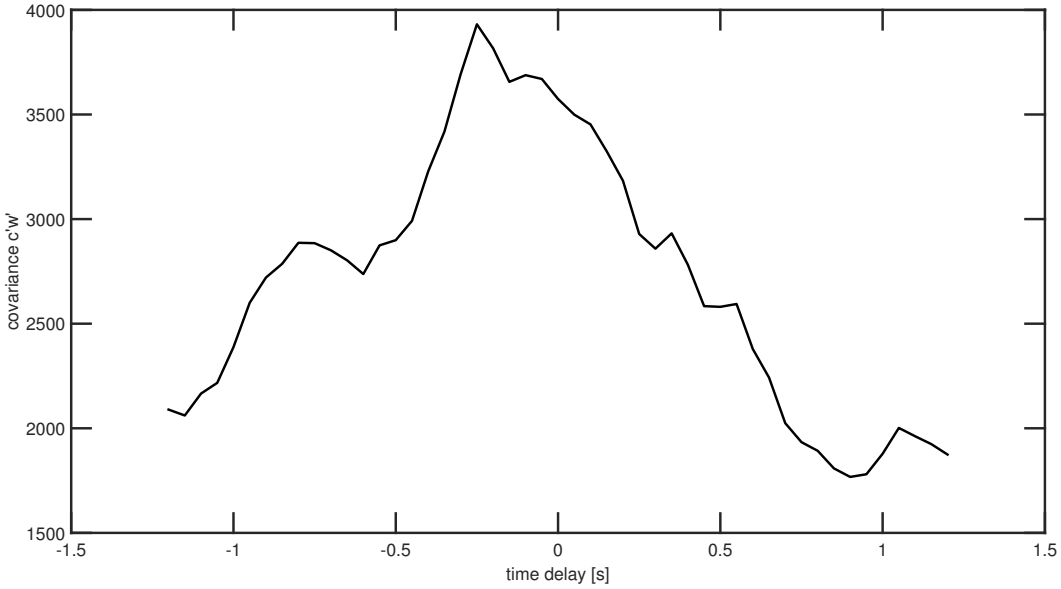

Figure 3. The delay offset vs the covariance c'w' between DMS and vertical wind speed. In this example the offset was set to -0.3 seconds. This means after calculating, using the valve switch, the time lag, between wind speed and concentration measurement, was still -0.3 s seconds.

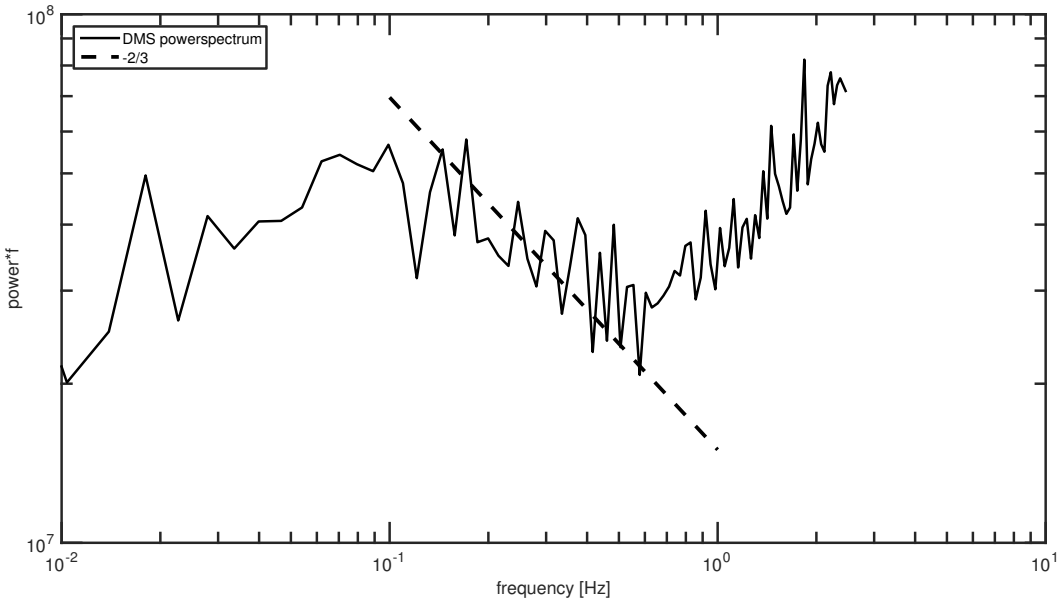

Figure 4. A sample power spectrum of the DMS concentration, recorded for 30 minutes. The dashed line is a reference to the $-\frac{2}{3}$ decay in the inertial subrange [*Kolmogorov*, 1941]. The increase after 1 Hz illustrates noise from the high frequency tubing loss and the instrument measurements.

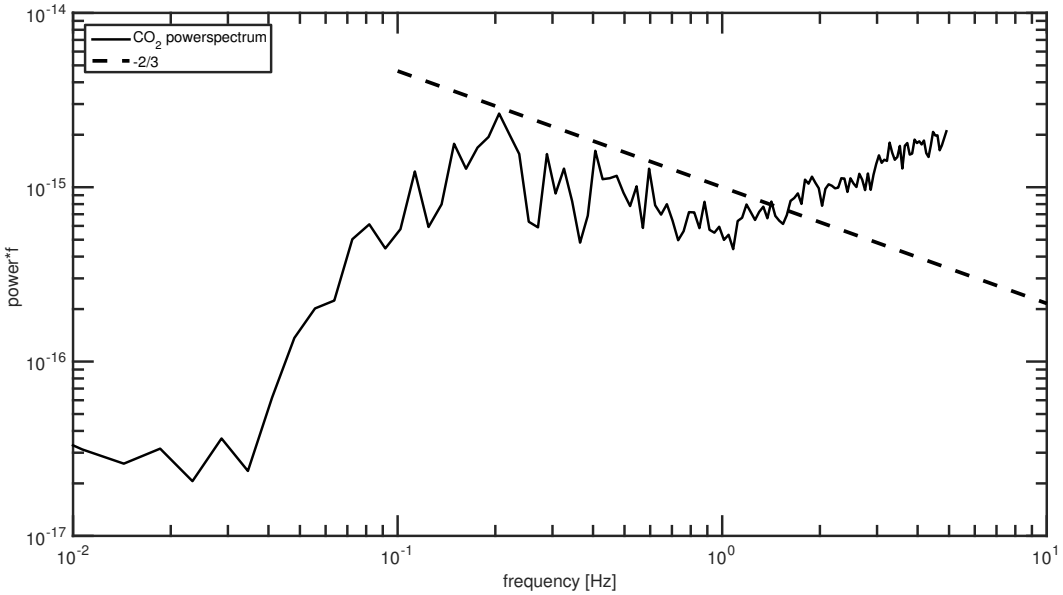

Figure 5. A sample power spectrum of the CO_2 concentration, recorded for 30 minutes. The dashed line is a reference to the $-\frac{2}{3}$ decay in the inertial subrange [*Kolmogorov*, 1941]. The increase after 1 Hz illustrates noise from the high frequency tubing loss and the instruments measurements.

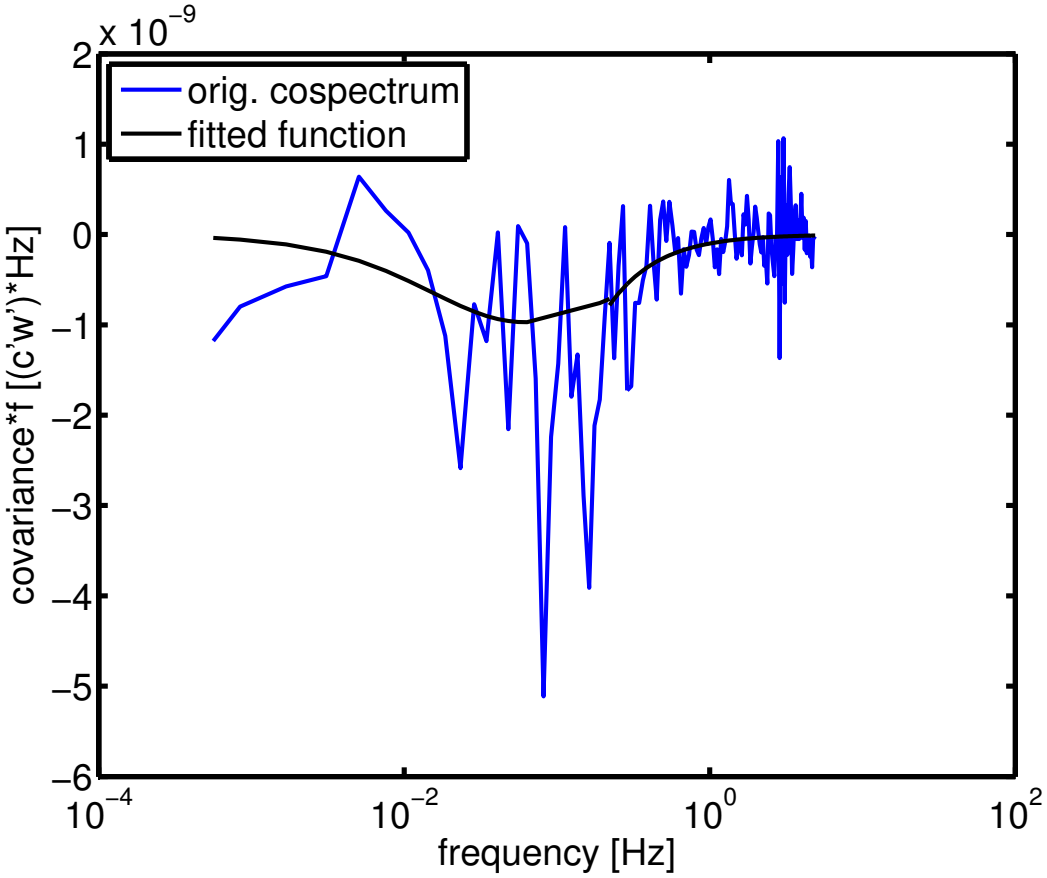

Figure 6. A sample CO_2 cospectrum (c'w'). The black line is a fit using an idealized function for scalar cospectra [*Kaimal et al.*, 1972].

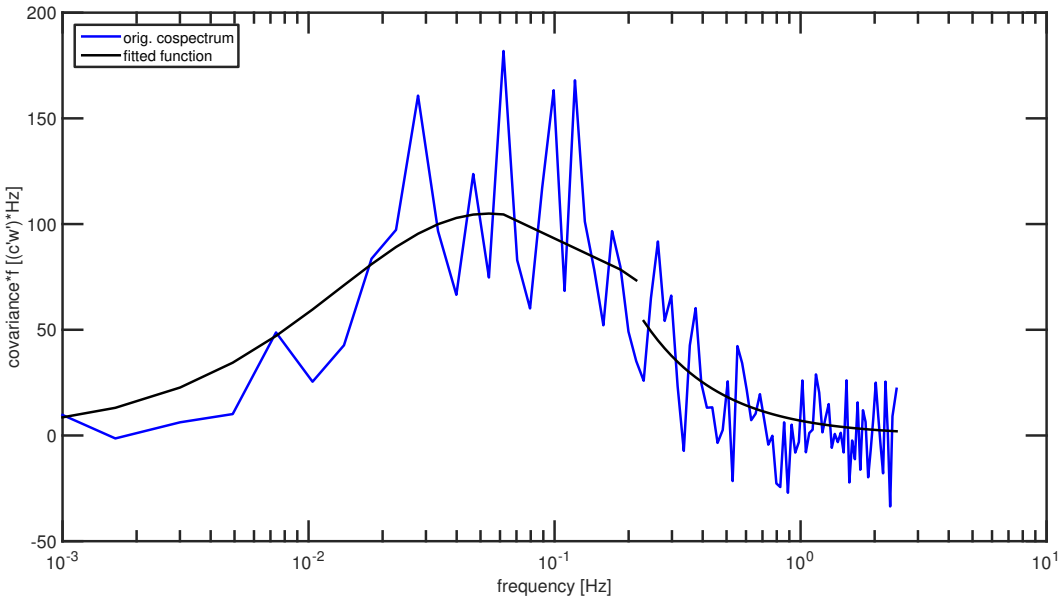

Figure 7. A sample DMS cospectrum (c'w'). The black line is a fit using an idealized function for scalar cospectra [*Kaimal et al.*, 1972].

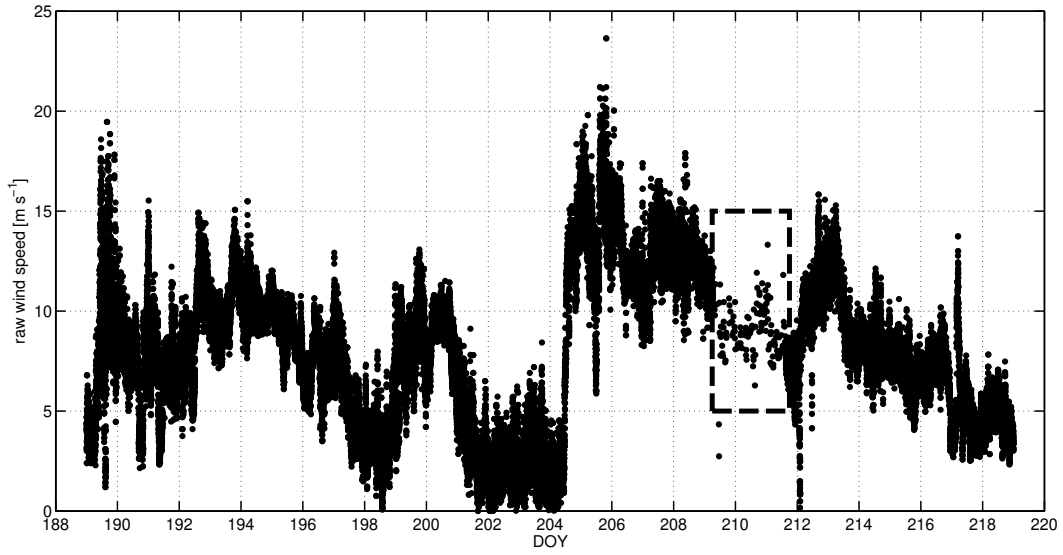

Figure 8. Uncorrected wind speed measured by the ship's meteorological station. The dashed rectangle indicates the time where data outages of the measurement system occurred. These outages were filled with data from the eddy covariance measurement system.

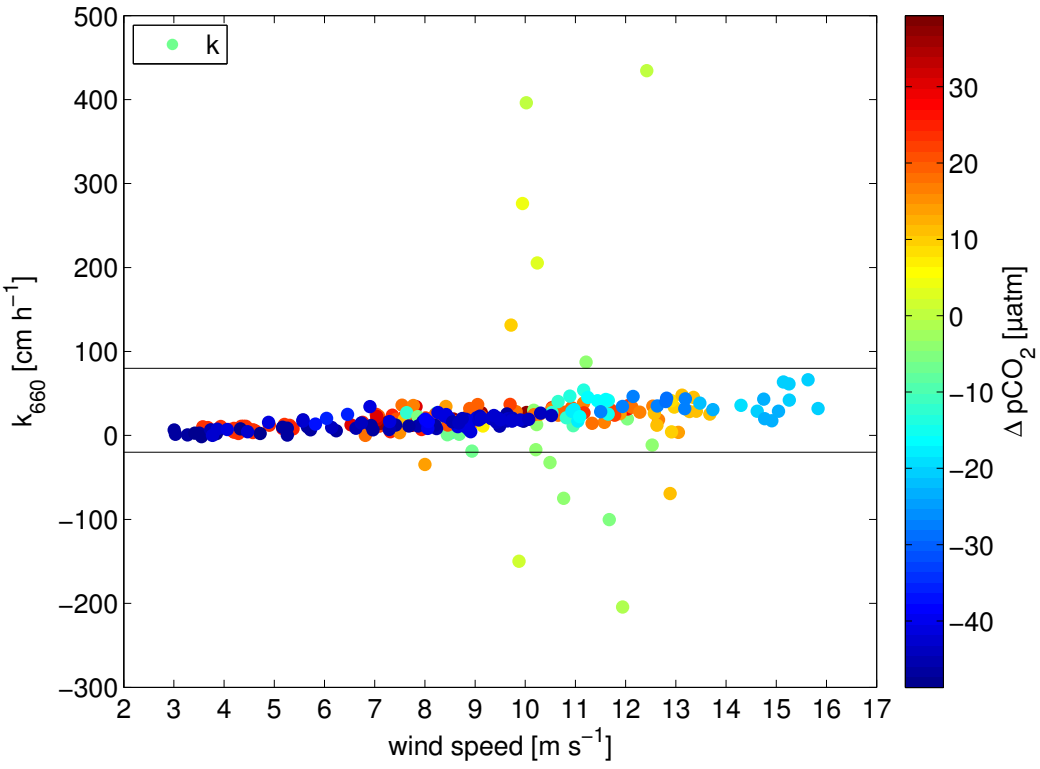

Figure 9. Complete CO_2 gas transfer velocity data set. Data below -20 cm h^{-1} and above 80 cm h^{-1} is discarded.